Bis(permethylpentalene)cerium – another ambiguity in lanthanide oxidation state

Andrew Ashley,[a] Gabor Balazs,[b] Andrew Cowley,[a] Jennifer Green,[b] Corwin H. Booth[c] and Dermot O'Hare*[a]

Received (in Cambridge, UK) 9th January 2007, Accepted 9th February 2007
First published as an Advance Article on the web 14th March 2007
DOI: 10.1039/b700303j

Ce(η^8-C_8Me_6)$_2$ exists in a valency close to Ce(III) with some Ce(IV) and provides an example of the Kondo effect in a discrete molecule.

The existence of cerocene [Ce(COT)$_2$; COT = cyclooctatetraene][1] has fascinated researchers for over 30 years. This material is remarkable in that it combines a notably strong oxidant (Ce^{IV}/Ce^{III} couple in $HClO_4$ is 1.30 V *vs.* Fc^+/Fc)[2] with a hydrocarbon dianion (reduction potential in HMPA −1.92 V *vs.* SCE).[3] The best way to classify the oxidation state of the metal in this complex remains the subject of much debate. Techniques that probe the electronic structure of the molecule as a whole,[4–8] or solely the Ce atom,[9–11] provide conflicting results. Interest has also been heightened in Ce(COT)$_2$ as a model to study the Kondo effect,[10] whereby a local magnetic moment spin polarises local conduction electrons thus forming a magnetic singlet. The physics associated with this phenomenon is essentially a 'particle in a box' which couples to a magnetic impurity; in cerocene this arises from the unusual valence of the metal atom (due to a multi-configurational electronic state) that acts as the latter whilst interacting with an unpaired spin on the COT ligands. A similar two configurational ground state for $[Ce(C_5H_5)_3]^+$ has been demonstrated experimentally by photoelectron spectroscopy.[12] This observation gives further insight into mixed-valence and heavy-fermion behaviour in intermetallic alloys and the study of transport and magnetic properties of quantum dots, carbon nanotubes and intermetallic nanoparticles.[10] Recently we reported a new permethylated pentalene ligand ($C_{14}H_{18}$; Pn*)[13,14] which can be regarded as isoelectronic with COT. In order to extend the applicability of Pn* to *f*-element chemistry, and because of our general interest in mixed-valence behaviour, we targeted the synthesis of Ce(Pn*)$_2$ in order to examine its electronic structure. In particular we were interested to see if this species would provide another rare example of the self-contained Kondo effect in a single molecule.

Although Cloke has briefly mentioned the synthesis of Ce(η^8-$Pn^{1,4\text{-}iPr3Si}$)$_2$ in a recent review,[15] no studies of its electronic structure have been reported to date. The reaction of $Li_2Pn^*(TMEDA)_x$ and $CeCl_3$ (2 : 1 ratio) in THF led to a brown solution, presumably containing solvated Li[Ce(Pn*)$_2$]. Attempted oxidation of this extremely air-sensitive solution with the oxidants commonly used to synthesise Ce(COT)$_2$ (*e.g.* allyl bromide or AgI) failed.[16] However, it was found that the use of excess 1,2-dichloroethane resulted in the smooth conversion to a vivid purple product. High-vacuum sublimation afforded Ce(η^8-Pn*)$_2$ (**1**) as an air-sensitive purple–black solid in moderate yield.†

Single crystals were grown from a saturated toluene solution at −78 °C. X-ray crystallography showed that each of the pentalene ligands is disordered over three positions related by a 120° rotation about the *c* axis. For a given orientation of one of the Pn* ligands of a molecule there are three possible symmetry-related orientations of the second. It is impossible to identify which of these is 'correct' by diffraction alone. Examination of space-filling models of the three possible structures suggests that none have unreasonably short contacts between non-bonded atoms and it is quite probable that a dynamic equilibrium exists within the crystal. One of the three orientations (Fig. 1) has an approximately staggered conformation, as illustrated by the interplanar angles between the two Ce1, C2 and C6 planes of 79.8°. The other two adopt skewed conformations (interplanar angles of 40.1° and 20.1°).

The geometry about the Ce centre deviates substantially from tetrahedral and the metal centre lies approximately equidistant from each C_5 ring of the pentalene ligand (2.30 Å from their best planes). The Pn* moiety is appreciably non-planar, with a fold-angle of 24.7°; this value compares with those reported for Ce(η^8-$Pn^{1,4\text{-}iPr3Si}$)$_2$ (26°) and the trivalent cerate [K(18-crown-6)(pyr)$_2$][Ce(η^8-$Pn^{1,4\text{-}iPr3Si}$)$_2$] (22°).[15] The average Ce–C bond length of 2.682 Å is similar to that found in Ce(COT)$_2$ (2.671 Å). The mean C–C distance within the bicyclo[3.3.0]octane ring of 1.43 Å is consistent with an aromatic π-system.

The room temperature solution phase ^{1}H NMR spectrum of **1** exhibits two sharp singlets in a 2 : 1 ratio at δ = 6.20 and 1.45 ppm respectively. The marked downfield resonance may be assigned to the C9, C11, C12, C14 methyl protons. The room temperature solution phase ^{13}C NMR displays five resonances (indicative of two orthogonal mirror planes bisecting the Pn* ligand) and also shows unusual chemical shifts for the aforementioned methyl

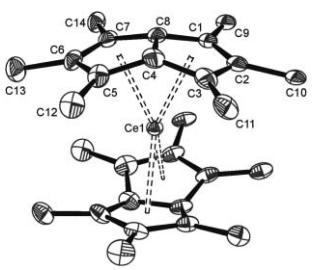

Fig. 1 X-ray structure of the staggered conformer of **1** (thermal ellipsoids shown at 50% probability, hydrogen atoms excluded for clarity).

[a]*Chemistry Research Laboratory, Mansfield Rd, Oxford, UK OX1 3TA. E-mail: dermot.ohare@chem.ox.ac.uk; Fax: 44 1865 285131; Tel: 44 1865 285130*
[b]*Inorganic Chemistry Laboratory, South Parks Rd, Oxford, UK OX1 3QR*
[c]*Chemical Sciences Division, Lawrence Berkeley National Laboratory, Berkeley, CA 94720, USA*

carbon atoms, which are moved upfield from the normal range to $\delta = 2.5$ ppm, yet the quaternary carbons to which they are bonded (C1, C3, C5 and C7) display a large shift in the opposite direction ($\delta = 149.9$ ppm). A sharp-lined NMR spectrum can be obtained from **1**, this suggests that the molecule is diamagnetic. However, the abnormal chemical shifts observed suggest a paramagnetic contribution to the shielding of some nuclei; it is not unusual for this to be manifested in only certain positions of a molecule whilst leaving others unaffected, due to the effects of unpaired spins being spatially directional as a consequence of orbital shapes (*vide infra*).[17] Variable temperature NMR between −100 °C and 80 °C shows no appreciable change in the chemical shifts, therefore any paramagnetic characteristic of the molecule is temperature-independent. The compound has been characterised further by IR spectroscopy, elemental analysis and high-resolution mass spectrometry.

Electrochemical measurements upon **1** show a fully reversible one-electron reduction at –830 mV *vs.* external Fc^+/Fc. This figure is unusually low for a Ce^{IV}/Ce^{III} couple and is very close to that obtained for $Ce(COT)_2$ (−800 mV *vs.* Fc^+/Fc).[16] This reversible addition of an electron to the molecule is consistent with a formal oxidation state of +IV for Ce, and the decrease in oxidative capability of Ce is undoubtedly due to the high degree of covalency within the complex.

Rare-earth L_{III}-edge X-ray absorption near-edge structure (XANES) spectroscopy is a common tool for determining *f*-occupancy, n_f, in intermediate valence systems.[10,18] For cerium atoms in such a case, the $|4f^0\rangle$ and $|4f^1\rangle$ configurations are nearly degenerate, and the ground state is $(1 - n_f)|4f^0\rangle + n_f|4f^1\rangle$. In formal Ce(IV) systems there is enough charge transfer between the ligand and the otherwise-unoccupied 4*f* orbital that the second term includes a contribution from $|\bar{L}\ 4f^1\rangle$ where $\bar{L}$ indicates a ligand hole. In CeO_2, for instance, n_f has been determined to be about 0.5, both from theoretical and experimental investigations.[19] When a 2*p* core hole ($\bar{2}\bar{p}$) is created with an X-ray, it interacts with the $4f^1$ components, splitting the states and creating distinct features in the XANES spectrum, allowing a fit of the features to determine the relative weights and therefore the *f*-occupancy.

The Ce L_{III}-edge XANES spectra were collected between 30 and 300 K in transmission mode on beamline 10-2 at the Stanford Synchrotron Radiation Laboratory (SSRL), and the sample was found to have an edge step corresponding to about 0.30 (Fig. 2). The two reference standards are the same as were used in Ref. 10: a Ce(III) standard of $Ce[N(SiMe_3)_2]_3$ and for Ce(IV) of Ce[5,7,12,14-Me_4-2,3:9,10-dibenzo[14]hexaenato$N_4(2^-)$]$_2$, [$Ce(tmtaa)_2$]. Ce(IV) systems are generally strongly mixed-valent

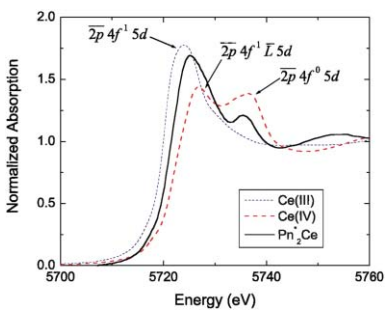

Fig. 2 Ce L_{III}-edge XANES data for **1**, with Ce^{III} and Ce^{IV} standards from Ref. 10 for comparison (data collected at 30 K).

as found for CeO_2,[19] and $Ce(tmtaa)_2$ has a comparable initial configuration which is a superposition of states, close to $^1/_2|f^0\rangle + {}^1/_2|\bar{L}\ 4f^1\rangle$.

With the assumption that the structure is due to initial state effects, the data were fitted to a combination of pseudo-Voigt functions. The first three pseudo-Voigts simulate the $\bar{2}\bar{p}4f^15d$, $\bar{2}\bar{p}4f^1\bar{L}5d$, and $\bar{2}\bar{p}4f^05d$ features (the 5*d* is the final state of the photoelectron). The latter feature is the most visually obvious for determining the presence of any tetravalent character. A fourth pseudo-Voigt is used as a rough model of the first extended X-ray absorption fine-structure oscillation just beyond 5740 eV, and is due to a structural effect.[20] Lastly, an integrated pseudo-Voigt is used to simulate the main edge step.

Taking the ratio of the tetravalent feature area to the total area of the first three pseudo-Voigts gives $n_f = 0.87 \pm 0.05$, where the uncertainty comes mostly from a strong correlation between the first two pseudo-Voigts. No change for n_f was observed within the measured temperature range and this is consistent with a strongly mixed-valent system; the value obtained for $Ce(\eta^8\text{-}COT)_2$ ($n_f = 0.89 \pm 0.03$) is strikingly similar (Fig. 2), suggesting that both compounds approximate more closely to trivalent cerium.

In order to examine the molecular orbital structure and investigate a possible origin of the unusual ^1H and ^{13}C NMR shifts found for **1**, a density functional theory (DFT) calculation was performed.‡ We note that such a calculation cannot reproduce the observed multiconfigurational ground state,[7,8] in contrast to a configuration interaction calculation, however DFT should be useful for identifying less subtle features and trends in the electronic structure. The bonding was analysed by fragment calculations and the complex symmetry was restrained to D_{2d} during geometry optimisation. Values of 2.67 and 1.42 Å were calculated for the mean Ce–C and C–C distances and the 24° for the ligand fold angle, in good agreement with the crystal structure data. The energy level diagram is depicted in Fig. 3 together with orbital topologies for key orbitals and their percentage character partitioned between metal and ligands.

The $8a_2$ HOMO and the $8b_1$ HOMO-1 resemble closely the e_{2u} and e_{2g} orbitals of $Ce(COT)_2$. On symmetry grounds the only possible Ce contribution to the $8a_2$ orbital is from an orbital of *f*

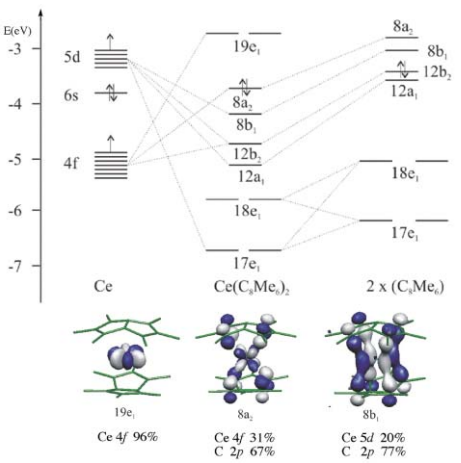

Fig. 3 Molecular orbital interaction diagram for **1** (only energy levels important for bonding are represented). Isosurfaces for key MOs and corresponding fragment interaction strengths depicted (H atoms are omitted from the structure for clarity).

symmetry. Thus in a multi-configuration description it is most likely that the antiferromagnetically coupled *f* electron and ligand hole are of a_2 symmetry. An intense and broad absorption in the UV–Visible spectrum (THF) is observed for **1** at λ_{max} = 530 nm (ε = 17000); the comparative feature for cerocene is 469 nm (ε = 8000). TDDFT calculations on **1** predict a low energy, intense transition (λ = 435 nm, f = 0.071) arising from excitation from the $8b_1$ orbital to a 4*f* orbital of a_2 symmetry. The intensity arises from the *d* to *f* character of the transition. The lower energy for the Pn* species is consistent with a more electron-rich characteristic of the ligand brought about from permethylation in comparison to COT, which decreases the HOMO–LUMO gap to 0.97 eV. This small separation also accounts for the TIP shown both by the magnetic measurements and the unusual chemical shifts. The extinction coefficient is also much higher and this is presumed to be a consequence of descent in symmetry from D_{8h} to D_{2d}, thereby making such a promotion more 'allowed'.

A noteworthy point is that atoms C1, C3, C5 and C7 have large coefficients in the $8a_2$ and $8b_1$ orbitals and it is these atoms which display the unusual NMR chemical shifts. It can be postulated that if a strongly mixed-valent system is in operation here (as the XANES data suggest), then the $4f^1$ contributions to the ground state of the molecule (and its attendant paramagnetism) are most likely to be experienced by these atoms, and thus these sites will experience a stronger perturbation through the contact shift (σ_p) term.[21]

The solid state magnetic susceptibility for $Ce(Pn^*)_2$ was measured between 4–300 K. The data show a small paramagnetic contribution at low temperature ("Curie tail"), which we have treated as an impurity contribution. A least-squares fit of this contribution to a Curie–Weiss expression gives C = 0.00350 emu·K mol^{-1} and θ = 2.2 K corresponding to approx. 0.9% of an S = 1/2 impurity. After correction for the diamagnetism of the quartz sampler holder and the diamagnetism of the electron cores **1** displays temperature independent paramagnetism (TIP) with $\chi(T) = (25.0 \pm 0.1) \times 10^{-4}$ emu mol^{-1}. This is somewhat larger than the TIP reported for $Ce(COT)_2$ ($\chi(T) = 1.4 \times 10^{-4}$ emu mol^{-1}). Following arguments in Ref. 10 and assuming both cerocene and $Ce(Pn^*)_2$ have the same effective *J*, this difference implies that the Kondo temperature scale is about 18 times smaller than cerocene, or around 600 K. Therefore, we expect below about 150 K that $\chi(T)$ should reach either a local or global maximum, and indeed $\chi(T)$ begins to fall off above this temperature. A decrease in temperature scale is expected from the decrease in the HOMO–LUMO gap, and is likely enhanced by the asymmetric bonding in $Ce(Pn^*)_2$, and should therefore reduce the total *f–p* hybridization strength.

In conclusion, a cerocene analogue, $Ce(\eta^8\text{-}Pn^*)_2$ has been studied using a variety of techniques including XANES spectroscopy and DFT calculations; the former gives strong evidence for a formal valency close to Ce(III) in this molecule and provides an example of the self-contained Kondo effect.

We acknowledge support from the EPSRC and the U.S. Department of Energy (DOE) under Contract No. DE-AC02-05CH11231.

Notes and references

† Reactions were carried out under N_2 atmosphere using dried solvents and Schlenk-line apparatus. THF (60 ml) was added to a mixture of $CeCl_3$ (0.79 g, 3.20 mmol) and $Li_2Pn^*(TMEDA)_{0.19}$ (1.43 g, 6.41 mmol) at room temperature and the reaction stirred for 24 h. To the resulting light brown suspension was added 1,2-dichloroethane (2.50 ml, 32.0 mmol) which led to the rapid formation of an intense purple coloured solution. The solvent was removed *in vacuo* and the residue extracted with CH_2Cl_2 (2 × 60 ml) and then filtered through Celite. The solvent was then stripped to leave a nearly black residue which was washed with pentane (2 × 30 ml). Sublimation at 180 °C, 10^{-6} mbar gave the product as a deep purple–black solid. Yield 0.99 g (1.95 mmol, 61% yield). Anal. Calc. for $C_{28}H_{36}Ce$: C 65.59, H 7.08. Found C 65.78, H 7.15%. MS (EI): *m/z* = 512 (83%, M^+), 326 (59%, $M^+ - Pn^*$), 186 (100%, Pn^*). ^{1}H NMR (C_6D_6, 300 K): δ 1.45 (6H, s); 6.20 (12H, s). ^{13}C {^{1}H} NMR (C_6D_6, 300 K): δ 2.5; 11.8; 108.5; 129.5; 149.9.

Crystal data: $C_{28}H_{36}Ce$, f.w. 512.71, crystal size 0.03 × 0.1 × 0.1 mm, trigonal, space group *R 32* with $a = b$ = 9.4931(3) Å, c = 22.1762(8) Å, V = 1730.75(10) Å^3, Z = 3, ρ_{calc} = 1.47 g cm^{-1}, $2\theta_{max}$ = 54.54°, λ = 0371073 Å, T = 150 K, total data 2932, unique data 520, μ = 1.98 mm^{-1}, 130 parameters, R_{int} = 0.0267, R_w = 0.0282. CCDC 633039. For crystallographic data in CIF or other electronic format see DOI: 10.1039/b700303j

‡ Computational data: The geometries were optimised with the GAUSSIAN program using the B3LYP functional and the 6-31++G* basis sets for C and H and Dunning/Huzinaga type basis set with the Stuttgart/Dresden pseudorelativistic core potential for Ce.[22] Fragment and TDDFT calculations were performed with the Amsterdam Density Functional (ADF) program package using the BP86 functional and TZP basis sets for all atoms.[23] The molecular orbitals of the molecule are constructed as linear combinations of the chosen fragments.

1 B. L. Kalsotra, R. K. Multani and B. D. Jain, *Chem. Ind. (London)*, 1972, 339.
2 N. G. Connelly and W. E. Geiger, *Chem. Rev.*, 1996, **96**, 877.
3 L. A. Paquette, C. D. Wright, III, S. G. Traynor, D. L. Taggart and G. D. Ewing, *Tetrahedron*, 1976, **32**, 1885.
4 A. Streitwieser, Jr., S. A. Kinsley, J. T. Rigsbee, I. L. Fragala and E. Ciliberto, *J. Am. Chem. Soc.*, 1985, **107**, 7786; A. Streitwieser, S. A. Kinsley, C. H. Jenson and J. T. Rigsbee, *Organometallics*, 2004, **23**, 5169.
5 N. Roesch and A. Streitwieser, Jr., *J. Am. Chem. Soc.*, 1983, **105**, 7237.
6 N. Roesch, *Inorg. Chim. Acta*, 1984, **94**, 297.
7 M. Dolg, P. Fulde, W. Kuechle, C. S. Neumann and H. Stoll, *J. Chem. Phys.*, 1991, **94**, 3011.
8 M. Dolg, P. Fulde, H. Stoll, H. Preuss, A. Chang and R. M. Pitzer, *Chem. Phys.*, 1995, **195**, 71.
9 N. M. Edelstein, P. G. Allen, J. J. Bucher, D. K. Shuh, C. D. Sofield, N. Kaltsoyannis, G. H. Maunder, M. R. Russo and A. Sella, *J. Am. Chem. Soc.*, 1996, **118**, 13115.
10 C. H. Booth, M. D. Walter, M. Daniel, W. W. Lukens and R. A. Andersen, *Phys. Rev. Lett.*, 2005, **95**, 267202.
11 H.-D. Amberger, H. Reddmann and F. T. Edelmann, *J. Organomet. Chem.*, 2005, **690**, 2238.
12 M. Coreno, M. de Simone, J. C. Green, N. Kaltsoyannis, N. Narband and A. Sella, *Chem. Phys. Lett.*, 2006, **432**, 17.
13 A. Ashley, A. R. Cowley and D. O'Hare, *Eur. J. Org. Chem.*, 2006, in press (DOI: 10.1002/ejoc.200700033).
14 A. Ashley, A. R. Cowley and D. O'Hare, *Chem. Commun.*, 2007, in press (DOI: 10.1039/b702150j).
15 O. T. Summerscales and F. G. N. Cloke, *Coord. Chem. Rev.*, 2006, **250**, 1122.
16 A. Streitwieser, S. A. Kinsley, C. H. Jenson and J. T. Rigsbee, *Organometallics*, 2004, **23**, 5169.
17 C. L. Honeybourne, *Nucl. Magn. Reson.*, 1978, **7**, 260.
18 J. L. Sarrao, C. D. Immer, Z. Fisk, C. H. Booth, E. Figueroa, J. M. Lawrence, R. Modler, A. L. Cornelius, M. F. Hundley, G. H. Kwei, J. D. Thompson and F. Bridges, *Phys. Rev. B: Condens. Matter*, 1999, **59**, 6855.
19 A. Kotani, T. Jo and J. C. Parlebas, *Adv. Phys.*, 1988, **37**, 37.
20 B. K. Teo, *EXAFS: Basic principles and Data Analysis*, Springer-Verlag, New York, 1986.
21 M. F. Rettig and R. S. Drago, *J. Am. Chem. Soc.*, 1969, **91**, 1361.
22 M. J. Frisch, *et al.*, *Gaussian 03*, *Revision C.02*, 2004, Gaussian Inc., Wallingford CT.
23 *ADF2004.01*, SCM, Theoretical Chemistry, Vrije Universitiet, Amsterdam, The Netherlands, http://www.scm.com.